J|A|C|S
ARTICLES
Published on Web 09/21/2002

Vapor−Liquid Interfacial Properties of Mutually Saturated Water/1-Butanol Solutions

Bin Chen,*,†,‡ J. Ilja Siepmann,‡ and Michael L. Klein†

Contribution from the Center for Molecular Modeling and Department of Chemistry, University of Pennsylvania, 231 S. 34th Street, Philadelphia, Pennsylvania 19104-6323, and Department of Chemistry and Department of Chemical Engineering and Materials Science, University of Minnesota, 207 Pleasant Street SE, Minneapolis, MN 55455-0431

Received May 31, 2002

Abstract: Adsorption and ordering at the vapor−liquid interfaces of mutually saturated water/1-butanol solutions at a temperature of 298.15 K were investigated using configurational-bias Monte Carlo simulations in the Gibbs ensemble and compared to the surface properties of neat water and 1-butanol liquids. A dense 1-butanol monolayer is observed at the surface of the water-rich phase, which results in a substantial decrease of its surface tension. In contrast, there is no enrichment of water molecules at the surface of the butanol-rich phase, and its surface tension is not significantly changed. Analysis of the interfacial structures reveals that these systems exhibit orientational ordering and composition heterogeneity. Analysis of the hydrogen-bonding distributions suggests that the formation of the 1-butanol monolayer is driven by an excellent match between water and the primary alcohol; that is, additional hydrogen bonds are formed between the excess free hydrogens of surface water and the excess hydrogen-bond acceptor sites of 1-butanol.

1. Introduction

The vapor−liquid interfaces of aqueous alcohol solutions exhibit one of the most intriguing surface phenomena: the formation of Langmuir monolayers.[1] The monolayer formation has been characterized by traditional surface tension and activity measurements.[2] Recently, much attention has been directed toward probing the molecular structure of these interfacial layers[3,4] because they are the key to the understanding of many important processes, including protein folding, membrane formation, micellar assembly, and wetting.[3f] Novel experimental techniques have been developed, including neutron and X-ray reflectometry and sum frequency vibrational spectroscopy. The former can be used in the determination of the thickness, density, and roughness of the surface layers,[4] while the latter provides information regarding the orientational ordering of molecules at interfaces.[3] However, the structural interpretation of these experiments is not always straightforward and often involves a reverse procedure using modeling methods. In addition, it should be noted that these techniques focus on average properties, but do not allow for a view of individual molecules.

In recent years, particle-based simulations have emerged as an alternative route to obtain microscopic structural information for many interfacial systems, including alcohol/water mixtures.[5] A critical issue for these molecular simulations is the choice of the appropriate statistical-mechanical ensemble for the investigation of these inhomogeneous systems.[5d] For immiscible liquids, the system is usually constructed by placing a layer of surface-active molecules with the experimentally determined surface coverage at the vapor−liquid interface. However, this surface coverage may not correspond to a stable phase for a given molecular force field. For miscible liquids, on the other hand, most simulations are started using a random mixture with a specified overall concentration, and the surface-active molecules are allowed to redistribute between the surface and interior parts of the simulated system. However, significant finite-size effects are present when these simulations are carried out in closed ensembles because the concentration in the interior

* To whom correspondence should be addressed. E-mail: binchen@cmm.chem.upenn.edu.
† University of Pennsylvania.
‡ University of Minnesota.

(1) (a) Franklin, B. *Philos. Trans. R. Soc. London* **1774**, *64*, 445. (b) Rayleigh, L. *Proc. R. Soc. London* **1890**, *47*, 364. (c) Langmuir, I. *J. Am. Chem. Soc.* **1917**, *39*, 1848.
(2) (a) Harkins, W. D.; Wampler, R. W. *J. Am. Chem. Soc.* **1931**, *53*, 850. (b) Addison, C. C. *J. Chem. Soc.* **1922**, 98. (c) Vochten, R.; Petre, G. *J. Colloid Interface Sci.* **1973**, *42*, 320. (d) Kahlweit, M.; Busse, G.; Jen, J. *J. Phys. Chem.* **1991**, *95*, 5580. (e) Gliński, J.; Chavepeyer, G.; Platten, J.-K.; Smet, P. *J. Chem. Phys.* **1998**, *109*, 5050.
(3) (a) Du, Q.; Superfine, R.; Freysz, E.; Shen, Y. R. *Phys. Rev. Lett.* **1993**, *70*, 2313. (b) Messmer, M. C.; Conboy, G. C.; Richmond, G. L. *J. Am. Chem. Soc.* **1995**, *117*, 8039. (c) Stanners, C. D.; Du, Q.; Chin, R. P.; Cremer, P.; Somorjai, G. A.; Shen, Y.-R. *Chem. Phys. Lett.* **1995**, *232*, 407. (d) Casson, B. D.; Braun, R.; Bain, C. D. *Faraday Discuss.* **1996**, *104*, 209. (e) Eisenthal, K. B. *Chem. Rev.* **1996**, *96*, 1343. (f) Scatena, L. F.; Brown, M. G.; Richmond, G. L. *Science* **2001**, *292*, 908. (g) Ju, S. S.; Wu, T. D.; Yeh, Y. L.; Wei, T. H.; Huang, J. Y.; Lin, S. H. *J. Chin. Chem. Soc.* **2001**, *48*, 625.
(4) (a) Li, Z. X.; Lu, J. R.; Styrkas, D. A.; Thomas, R. K.; Rennie, A. R.; Penfold, J. *Mol. Phys.* **1993**, *80*, 925. (b) Li, Z. X.; Lu, J. R.; Thomas, R. K.; Rennie, A. R.; Penfold, J. *J. Chem. Soc., Faraday Trans.* **1996**, *92*, 565. (c) Yano, Y. F. *J. Chem. Phys.* **2002**, *116*, 8093.
(5) (a) Gao, J.; Jorgensen, W. L. *J. Phys. Chem.* **1988**, *92*, 5813. (b) Matsumoto, M.; Kataoka, Y. *J. Chem. Phys.* **1989**, *90*, 2398. (c) Matsumoto, M.; Takaoka, Y.; Kataoka, Y. *J. Chem. Phys.* **1993**, *98*, 1464. (d) Tarek, M.; Tobias, D. J.; Klein, M. L. *J. Chem. Soc., Faraday Trans.* **1996**, *92*, 559. (e) Tarek, M.; Bandyopadhyay, S.; Klein, M. L. *J. Mol. Liq.* **1998**, *78*, 1. (f) Sokhan, V. P.; Tidesley, D. J. *Faraday Discuss.* **1996**, *104*, 193. (g) Wilson, M. A.; Pohorille, A. *J. Phys. Chem. B* **1997**, *101*, 3130.

10.1021/ja027130n CCC: $22.00 **© 2002 American Chemical Society**

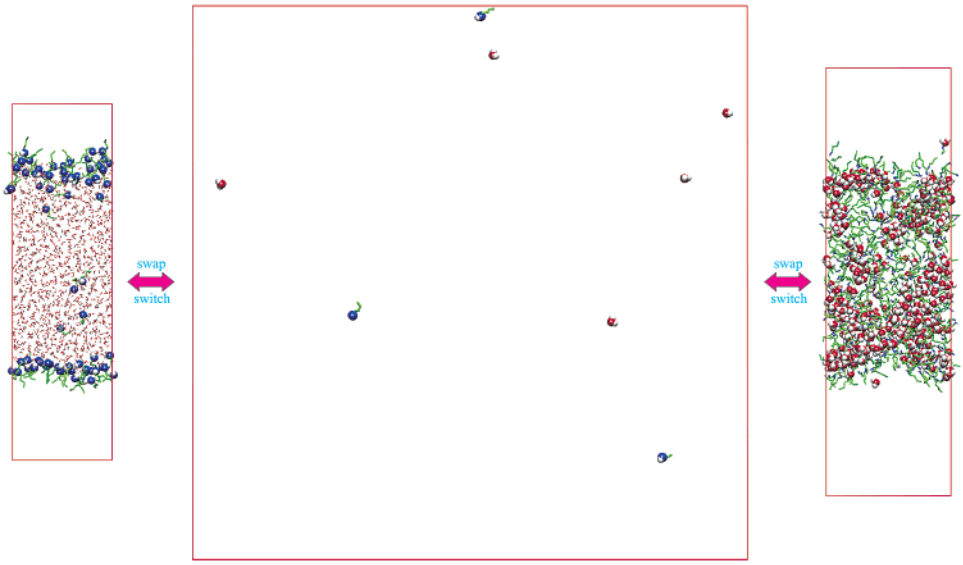

Figure 1. Setup of the Gibbs ensemble Monte Carlo simulations. The elongated boxes on the left and right show the mutually saturated water and 1-butanol liquid phases, respectively, while the cubic box in the middle contains the saturated vapor phase. Polar hydrogens, water oxygens (highlighted in the 1-butanol-rich phase), butanol oxygens (highlighted in the water-rich phase), and methyl/methylene groups are depicted in white, red, blue, and green, respectively.

part of the film differs from the specified overall concentration due to surface enrichment or depletion. Most important, neither of these approaches allows one to determine the properties of saturated solutions. Thus, it is more advantageous (but technically more difficult) to carry out the simulations in an open ensemble, such as the Gibbs[6] or grand canonical ensemble,[7] because they allow precise control of the bulk concentration of the surface-active species. Furthermore, investigations of mutually saturated solutions are straightforward in the Gibbs ensemble.[6d,e]

The focus of this work are the vapor−liquid interfaces of mutually saturated water/1-butanol mixtures which were previously examined using surface tension measurements[2] and neutron reflection studies.[4b] The remainder of this article is arranged as follows. Section 2 describes the simulation details. Thereafter, we present simulation results and discussions in section 3. Finally, conclusions are outlined in section 4.

2. Simulation Details

A combination of the Gibbs ensemble Monte Carlo (GEMC)[6] and coupled-decoupled configurational-bias Monte Carlo (CBMC)[8] techniques is used here. Simulations in the Gibbs ensemble involve at least two phases that are treated using separate, but thermodynamically connected, simulation boxes. Figure 1 illustrates the Gibbs ensemble setup (one vapor and two liquid phases) employed to investigate the vapor−liquid interfaces of the saturated water/1-butanol mixtures. The boxes that contain the liquid phases are elongated along one axis to create the vapor−liquid interfaces.[9] In this setup, the overall numbers of water and 1-butanol molecules, the combined volume of the three simulation boxes, the interfacial area of each of the two liquid-phase boxes, and the temperature are held constant. The constant interfacial area is not a thermodynamic constraint in the usual sense and influences only the distribution of molecules between the bulk liquid and interfacial liquid. Thus, once the temperature as the independent variable is set (for this system with two components and three phases), molecules and volume need to be distributed over the three simulation boxes to reach equilibrium (compositions of the three phases and saturated vapor pressure).

Particle transfers are carried out using CBMC swap moves.[8,10] The vapor-phase box helps to facilitate the transfer of molecules between the two liquid phases because it avoids the concurrent energetic penalties associated with the removal and insertion of a molecule from/into liquid phases.[6d] In addition to CBMC swap moves of entire molecules[10] (which attempt to transfer a molecule from one phase to another, thereby equalizing the chemical potentials of this species between the two phases), CBMC switch moves[11] are also used for partial particle exchanges. In the latter move, two molecules of different types but containing a common functional group are selected, and their identities are switched through regrowing of the structural differences. The switch move has a much higher acceptance rate than the regular CBMC swap move of larger molecules (e.g., 1-butanol here) and is used to equalize the differences in chemical potentials of different species. As should be expected, the acceptance rate of this move depends on the similarity between the two molecule types. Considering the relatively large size difference between water and 1-butanol, a few intermediates (methanol, ethanol, and 1-propanol) are added to the system, and the CBMC switch moves are targeted at the deletion/addition of a single methylene unit (yielding an acceptance rate that is about 3 orders of magnitude higher than that for the direct water/1-butanol switch). The overall number of intermediate molecules (or their concentrations) needs to be kept very low,

(6) (a) Panagiotopoulos, A. Z. *Mol. Phys.* **1987**, *61*, 813. (b) Panagiotopoulos, A. Z.; Quirke, N.; Stapleton, M.; Tildesley, D. J. *Mol. Phys.* **1988**, *63*, 527. (c) Smit, B.; de Smedt, Ph.; Frenkel, D. *Mol. Phys.* **1989**, *68*, 931. (d) Canongia Lopes, J. N.; Tildesley, D. J. *Mol. Phys.* **1997**, *92*, 187. (e) Chen, B.; Siepmann, J. I. *J. Am. Chem. Soc.* **2000**, *122*, 6464.
(7) (a) Norman, G. E.; Filinov, V. S. *High Temp. Res. USSR* **1969**, *7*, 216. (b) Adams, D. J. *Mol. Phys.* **1974**, *28*, 1241.
(8) (a) Siepmann, J. I.; Frenkel, D. *Mol. Phys.* **1992**, *75*, 59. (b) Frenkel, D.; Mooij, G. C. A. M.; Smit, B. *J. Phys.: Condens. Matter* **1992**, *4*, 3053. (c) Martin, M. G.; Siepmann, J. I. *J. Phys. Chem. B* **1999**, *103*, 4508.
(9) Chen, B.; Siepmann, J. I.; Klein, M. L. *J. Phys. Chem. B* **2001**, *105*, 9840.
(10) Mooij, G. C. A. M.; Frenkel, D.; Smit, B. *J. Phys.: Condens. Matter* **1992**, *4*, L255.
(11) (a) Martin, M. G.; Siepmann, J. I. *J. Am. Chem. Soc.* **1997**, *119*, 8921. (b) Siepmann, J. I.; McDonald, I. R. *Mol. Phys.* **1992**, *75*, 255.

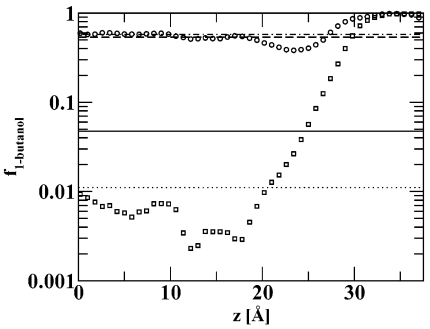

Figure 2. Symmetrized composition profiles (calculated from molecular center-of-mass positions and averaged over the two interfaces of a given liquid slab) for the saturated water and butanol phases shown as □ and ○, respectively. For comparison, the average compositions of these liquid slabs are illustrated by solid and dashed lines, respectively, and the bulk saturation concentrations (obtained from simulations without explicit interfaces) are shown as dotted and dashed−dotted lines, respectively.

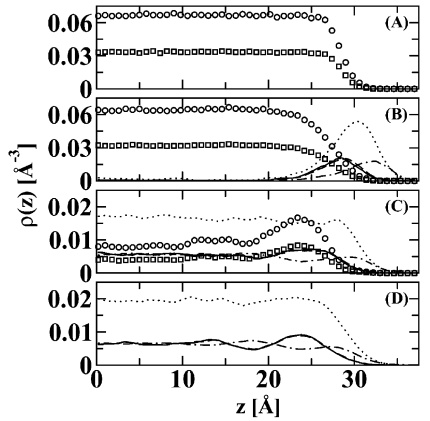

Figure 3. Symmetrized number density profiles: (A) neat water phase; (B) saturated water phase (butanol densities are multiplied by a factor of 3); (C) saturated 1-butanol phase; (D) neat 1-butanol phase. The values for water oxygen and hydrogen are depicted by □ and ○, respectively, while those for the hydroxyl hydrogen, hydroxyl oxygen, methylene, and methyl groups of 1-butanol are depicted as solid, dashed, dotted, and dashed−dotted lines.

so that these "impurities" have a negligible effect on the phase properties. In the simulations described here, only 2 methanol, 2 ethanol, and 2 1-propanol intermediates were used, while the system contained 1728 water and 480 1-butanol molecules.

The interactions of the water and alcohol molecules are described by the nonpolarizable TIP4P (transferable intermolecular potentials-4 points)[12] and TraPPE-UA (transferable potentials for phase equilibria-united atom)[13] force fields, respectively. In these models, the nonbonded interactions are described by pairwise-additive Lennard-Jones 12−6 potentials and Coulombic interactions of fixed partial charges. Spherical potential truncations at 14 Å were used for the Lennard-Jones interactions. In addition, an Ewald sum with tin-foil boundary conditions was used to treat the long-range electrostatic interactions.[14]

The CBMC/GEMC simulations were carried out at 298.15 K for three systems: neat water, neat 1-butanol, and mutually saturated water/1-butanol. All simulations were initially started using bulk liquid phases (i.e., without vapor−liquid interfaces). After the densities and compositions (only for the binary mixture) of the two phases (for the neat systems) or three phases (for the binary mixture) reached saturation, the simulation boxes which contained a liquid phase were duplicated along one of the three Cartesian axis and then further elongated to create the vapor−liquid interfaces. Thus, three independent starting configurations (duplication along *x*, *y*, or *z* axis) were created for each system. The final system sizes were 1500 molecules for neat water, 300 molecules for neat 1-butanol, and 2214 molecules for the mutually saturated water/1-butanol system (1728 water, 480 1-butanol, 2 methanol, 2 ethanol, and 2 1-propanol molecules). Each individual system was further equilibrated for more than 10^4 Monte Carlo cycles (10^5 Monte Carlo cycles for the mixture). The production periods consisted of 2×10^5, 6×10^5, and 3×10^5 Monte Carlo cycles for neat water, neat 1-butanol, and mutually saturated water/1-butanol, respectively. The statistical uncertainties were estimated from the three independent simulations.

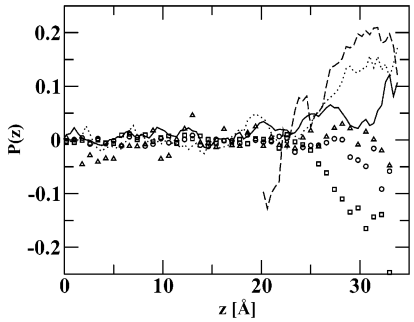

Figure 4. Comparison of the symmetrized orientational order parameter profiles for water (symbols) and 1-butanol (lines) in the neat (□ and solid), saturated water (○ and dashed), and saturated butanol (△ and dotted) phases.

3. Simulation Results and Discussions

A. Surface Tension and Surface Excess. The surface tension is the most important thermodynamic property for interfaces and can be directly calculated from a simulation as follows:[14b,15]

$$\gamma = \frac{1}{2A}\langle 2W_{zz} - W_{xx} - W_{yy}\rangle + \gamma_{\text{tail}} \qquad (1)$$

where the angular brackets denote an ensemble average, $A = 2L_xL_y$ is the total surface area, W_{xx}, W_{yy}, and W_{zz} are the molecular virial tensors, and γ_{tail} is the tail correction for the truncated part of the LJ interactions. The calculated surface tensions are 56 ± 3 mN/m for neat water (in good agreement with previous simulation results[5c] for the TIP4P model of 50 mN/m not including γ_{tail}), 23 ± 2 mN/m for neat 1-butanol, 37 ± 3 mN/m for 1-butanol-saturated water, and 25 ± 3 mN/m for water-saturated 1-butanol. The corresponding experimental results for water, 1-butanol, and 1-butanol-saturated water are 72,[16] 24,[16] and 28 mN/m,[2] respectively. The deviations are appreciable for the neat and saturated water phases. However,

(12) Jorgensen, W. L.; Chandrasekhar, J.; Madura, J. D.; Impey, R. W.; Klein, M. L. *J. Chem. Phys.* **1983**, *79*, 926.
(13) (a) Martin, M. G.; Siepmann, J. I. *J. Phys. Chem. B* **1998**, *102*, 2569. (b) Chen, B.; Potoff, J. J.; Siepmann, J. I. *J. Phys. Chem. B* **2001**, *105*, 3093.
(14) (a) Allen, M. P.; Tildesley, D. J. *Computer Simulation of Liquids*; Oxford University Press: New York, 1989. (b) Alejandre, J.; Tildesley, D. J.; Chapela, G. A. *J. Chem. Phys.* **1995**, *102*, 4574.
(15) (a) Rowlinson, J. S.; Widom, B. *Molecular Theory of Capillarity*; Clarendon: Oxford, 1992. (b) Salomons, E.; Mareschal, M. *J. Phys.: Condens. Matter* **1991**, *3*, 3645.
(16) Lide, D. A. *CRC Handbook of Chemistry and Physics*; CRC Press: Boca Raton, FL, 1991.

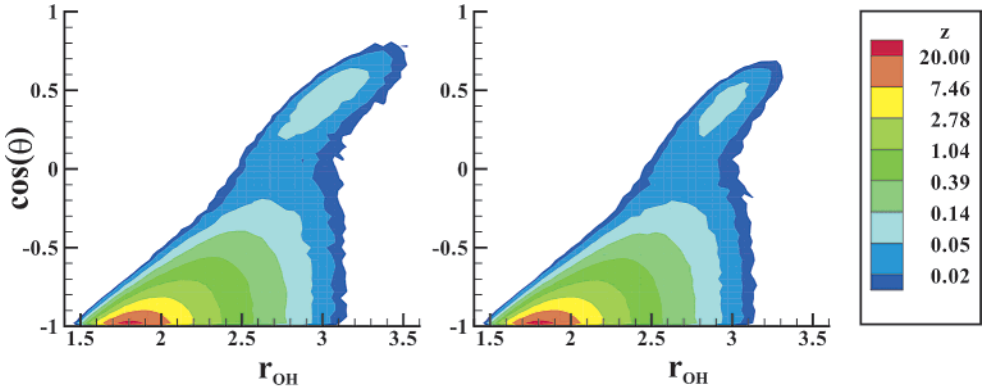

Figure 5. Contours of the two-dimensional distribution function of the O···H distance and of the cosine of the O···HO angle averaged over all pairs of water hydrogen and its nearest intermolecular oxygen in the phase. The results for pure water and the 1-butanol-saturated water are shown in the left and the right panel, respectively.

the simulation yielded a much lower saturation concentration of $x_{\text{butanol}} = 0.011 \pm 0.001$ (obtained using a system without explicit interfaces) as compared to the experimental result of 0.019.[2c,d,e] In fact, the calculated surface tension agrees much better with the experimental result of 35 mN/m for $x_{\text{butanol}} = 0.011$.[2d,e] Obviously, significant improvements in the force fields are needed to allow for quantitative predictions of surface tensions, but at least the results for 1-butanol modeled with the TraPPE-UA force field are more encouraging.

Although the 1-butanol saturation leads to a significant decrease of the surface tension of the water-rich phase, little change upon water saturation is observed for the butanol-rich phase. Already the snapshots shown in Figure 1 yield a first visual explanation that the existence (or lack thereof) of significant surface composition enhancements is responsible for the observed differences between the water- and butanol-rich phases. The local 1-butanol compositions for these two phases are depicted in Figure 2. For both phases, the surfaces are almost exclusively populated by 1-butanol molecules ($x_{\text{butanol}} > 0.95$), followed by a 1-butanol depleted region, before approaching the bulk saturation concentration (found from a simulation without explicit interfaces). The existence of a "depletion layer" was also noticed by Tarek et al. for ethanol/water solutions.[5d,e] Again, it needs to be reiterated that the concentration in a finite liquid slab (averaged over a single liquid-slab simulation box) differs substantially from the bulk saturation concentration (e.g., by about a factor of 4 for the 1-butanol-saturated water phase), thus illustrating the need to carry out these simulations in the Gibbs ensemble.

Number density profiles for individual (pseudo-)atoms are shown in Figure 3. The formation of the dense 1-butanol monolayer in the saturated water phase can be seen from the distinct peaks at $z \approx 30$ Å. In particular, the peaks for the hydroxyl oxygen and hydrogen are nearly symmetric with a Gaussian shape, whereas the peaks for the methyl and methylene groups are wider and show significant tailing toward the aqueous phase. Furthermore, the individual peak heights for all 1-butanol (pseudo-)atoms in the saturated water phase are comparable to the densities observed for neat 1-butanol, a clear indication for the formation of a rather dense monolayer and an explanation for the similarity in the surface tensions of the saturated water and butanol phases. The surface excess, Γ_e, of 1-butanol can be calculated from the density profiles in two different ways, either by directly integrating the area under the monolayer peaks or through the following equation:[5e]

$$\Gamma_e = \frac{\sqrt{\pi}\sigma\rho_{\max}}{2N_A} \tag{2}$$

where σ is the full width at $1/e$ of the peak height, $\rho_{\max}$, and N_A is Avogadro's number. Both methods yield a value of 6.6×10^{-10} mol/cm^2, which is in the range of the experimentally determined saturation values: 5.9×10^{-10} mol/cm^2 from surface tension measurements[2c,e] and 6.9×10^{-10} mol/cm^2 from neutron reflection studies.[4b] The corresponding molecular areas, given by $1/\Gamma_e N_A$, are 25, 28, and 24 Å^2, respectively. From the density profiles, a thickness of $\sigma = 6.6$ Å is estimated for the butanol headgroup, and a value of 7.8 Å is estimated for the tail segments. Either value is much lower than the 18 Å obtained from neutron reflection studies.[4b] However, this experimental value also contains the contribution from the capillary wave roughness. The wavelengths of capillary fluctuations are much longer than the lateral size of our simulation cells. For example, capillary waves with wavelengths ranging from 400 to 80 000 Å have been estimated by Schwartz et al. for the water−vapor interface.[17]

Although the surfaces of the neat and water-saturated 1-butanol phases do not show large surface excesses, it should nevertheless be noted that, particularly for the alcohol headgroup, there are substantial density oscillations near the surface. The outermost region of the surfaces is populated mostly by the butanol tails, leading to the high headgroup density about 5 Å toward the interior. The high headgroup density in this region is presumably responsible for the appreciably higher water mole fraction (see Figure 1) in this part of the saturated 1-butanol phase.

The distributions of the 1-butanol peaks in the saturated water phase show a similar arrangement with the position of the methyl peak about 4 Å further out than the oxygen and hydrogen peaks. Noteworthy is also that the width of the water surface increases substantially from neat water to butanol-saturated water, with 90−10 widths of 4.4 and 6.4 Å, respectively.

B. Surface Ordering. In addition to the composition heterogeneity, the orientational ordering of anisotropic molecules

(17) Schwartz, D. K.; Schlossman, M. L.; Kawamoto, E. H.; Kellog, G. J.; Pershan, P. S.; Ocko, B. M. *Phys. Rev. A* **1990**, *41*, 5687.

is an important structural characteristic of surfaces and interfaces. Different systems exhibit different types of ordering. For example, water tends to have its dipole aligned flat at the water/air surface,[18] while in Langmuir monolayers of alcohols and fatty acids the alkyl chains stand preferentially upright.[3c,d] The ordering behavior is conveniently described by an orientational order parameter defined by the angle θ between the surface normal and some internal vectors of the molecule as follows:[19]

$$P(z) = \frac{1}{2}\langle 3(\cos^2\theta) - 1\rangle \quad (3)$$

For a random (isotropic) system, P is near zero, whereas $P = -1/2$ represents a system with all of the vectors parallel to the interface, and $P = 1$ represents a system with all of the vectors perpendicular to the interface. The ordering of water is best represented by its dipole vector. For 1-butanol, the internal vectors are chosen to be those connecting a pair of carbon atoms that are separated by two bonds.

The orientational order parameters of the water and 1-butanol molecules in the neat and saturated phases are plotted in Figure 4. For neat water, P has a large negative value at the surface, demonstrating a strong tendency for the water dipoles to align parallel to the interface. This surface ordering, however, becomes much weaker when water is covered by the 1-butanol monolayer and vanishes completely for the water-saturated 1-butanol phase. For 1-butanol, the P values near the surface are positive (chains standing upright). The magnitude of P for butanol is much larger for the saturated water phase, which is covered by a well-organized monolayer, than for the neat 1-butanol phase, and the saturated 1-butanol phase falls in between. The ordering of 1-butanol differs significantly from those for neat alkanes which preferentially align parallel to the surface.[20] Despite that the alkyl chains of 1-butanol show orientational ordering for the surface monolayer, the torsional angle distributions (or the population of the gauche defects) remain close to those for neat liquid 1-butanol. For example, there is only a minor increase in the trans population of the CCCC dihedral angle (neat 1-butanol: $f_t = 0.709$, $f_{g+} = 0.145$, and $f_{g-} = 0.146$; 1-butanol monolayer: $f_t = 0.719$, $f_{g+} = 0.141$, and $f_{g-} = 0.140$). Earlier simulation studies by Gao and Jorgensen[5a] showed a substantial increase in the trans population of the CCCC dihedrals for a closed-packed 1-hexanol monolayer on water. As discussed in section 3.A, we observe that the packing density of 1-butanol molecules in the monolayer is about 20% below close packing for alkyl tails; that is, there is sufficient room for the 1-butanol tails to exhibit conformational disorder.

C. Surface Hydrogen Bonding. Many experimental and modeling studies[3a,f,21] have yielded evidence for free dangling OH bonds at the water/air surface. To quantify the density of these free hydrogens (FH), the following analysis is employed here: for each water hydrogen, the closest intermolecular oxygen is located, and the O···H distance and the O···HO angle are used to construct two-dimensional histograms. Compared in Figure 5 are the hydrogen-bonding patterns for the neat water and 1-butanol-saturated water phases. For both systems, two distinct domains are present in these histograms: one at 1.5 Å $< r_{OH} <$ 2.5 Å and $-1 < \cos\theta_{OH\cdots O} < -0.4$ and the other at 2.5 Å $< r_{OH} <$ 3.5 Å and $0 < \cos\theta_{OH\cdots O} < 1$, which correspond to hydrogen-bonded and free hydrogens, respectively. However, the density of the FH domain in the saturated phase is significantly reduced as compared to that in neat water. By integrating the area under the FH domain, the fraction of FHs, f_{FH}, can be obtained, and the absolute FH number at the water/air surface is calculated by correcting for the bulk contribution

$$N_{FH} = N^{tot} \times f_{FH} - N^{bulk} \times f_{FH}^{bulk} \quad (4)$$

where N^{tot} is the total number of water hydrogens, N^{bulk} is the number of bulk hydrogens (bulk is defined as a region where the density is above 95% of the average density of the interior part of the phase), and f_{FH}^{bulk} is the fraction of "free hydrogens" in the bulk (estimated from simulations of bulk liquid phases without any interface). Dividing N_{FH} by the surface area yields the FH number density: 2.0×10^{14} cm^{-1} for water and 0.9×10^{14} cm^{-1} for the 1-butanol-saturated water. Thus, the formation of the 1-butanol monolayer at the water surface causes a substantial decrease of FHs. These findings are in excellent agreement with spectroscopic measurements that yielded a FH density of $\sim 2.7 \times 10^{14}$ cm^{-1} for the neat water/air surface and a substantial reduction of the free OH stretch intensity when water is covered by a full alcohol monolayer.[3a]

For water, the decrease in FHs leads directly to a gain in the total number of hydrogen bonds. From integrating over the hydrogen-bonded domain (1.5 Å $< r_{OH} <$ 2.5 Å and $-1 < \cos\theta_{OH\cdots O} < -0.4$; see Figure 5) and subtracting the bulk contribution, it is found that a water molecule at the neat water/air surface is on average involved in 3.14 hydrogen bonds. This number increases to 3.51 for the 1-butanol-saturated water phase. Further hydrogen-bond analysis shows that the number of hydrogen bonds per 1-butanol molecule also increases from 1.94 in its neat phase to 2.21 for the monolayer at the surface of the saturated water phase. A number close to 2 found for the pure phase is a result of the formation of predominantly linear hydrogen-bonded aggregates, whereas a number greater than 2 for the monolayer arises from the fact that each 1-butanol oxygen can act as a hydrogen-bond acceptor for more than one hydrogen. Indeed, the total number of accepted hydrogen bonds for the hydroxyl oxygen in the butanol monolayer is 1.28, of which 1.10 is donated by water molecules. Therefore, both water and 1-butanol benefit from the formation of the monolayer structure through the gain of hydrogen bonds between free surface hydrogens of water and the excess hydrogen-bond acceptors of 1-butanol. This type of cooperativity can only happen at the interface, and it also encourages segregation of water and 1-butanol, which explains the depletion of 1-butanol below the surface of the saturated water and butanol phases.

4. Conclusions

The combination of configurational-bias and Gibbs ensemble Monte Carlo techniques allows for the first simulations that probe the surface properties of mutually saturated water/alcohol solutions. In this work, the vapor−liquid surfaces of neat water, neat 1-butanol, and their saturated solutions at $T = 298.15$ K

(18) Townsend, R. M.; Gryko, J.; Rice, S. A. *J. Chem. Phys.* **1985**, *82*, 4391.
(19) Harris, J. G. *J. Phys. Chem.* **1992**, *96*, 5077.
(20) Chen, B.; Siepmann, J. I.; Oh, K. J.; Klein, M. L. *J. Chem. Phys.* **2002**, *116*, 4317.
(21) (a) Eggebrecht, J.; Gubbins, K. E.; Thompson, S. M. *J. Chem. Phys.* **1987**, *86*, 2286. (b) Wilson, M. A.; Pohorille, A.; Pratt, L. R. *J. Phys. Chem.* **1987**, *91*, 4873. (c) Matsumoto, M.; Kataoka, Y. *J. Chem. Phys.* **1988**, *88*, 3233. (d) Townsend, R. M.; Rice, S. A. *J. Chem. Phys.* **1991**, *94*, 2207.

were investigated. It was found that the interfacial properties of water are modified dramatically in the presence of amphiphilic 1-butanol, whereas the changes are less significant for the saturated butanol phase. The calculated surface tension of the water phase decreases by about 35% upon saturation with 1-butanol, while the corresponding experimental decrease is about 60%, which is related to the underprediction of the 1-butanol solubility in the simulation. The surface tension lowering is caused by the formation of a dense 1-butanol monolayer with a calculated surface coverage of 25 Å^2 per molecule, comparable to the experimental estimates that range from 24 to 28 Å^2 per molecule. Thus, it is evident that the current simulations can yield a semiquantitative picture of the surface properties of saturated water−alcohol solutions. We would like to argue that polarizable force fields[22] and the associated increase in computational complexity will be required to achieve quantitative predictions for the intricate interplay of bulk partitioning and surface adsorption found in these systems.

Analysis of the microscopic structures reveals that the surfaces of these systems exhibit various types of ordering and heterogeneity. At the surface, the water dipoles tend to align parallel to the surface, whereas the alkyl chains of 1-butanol prefer to stand upright. Interestingly, the presence of the 1-butanol monolayer leads to a decrease in the orientational ordering of the water dipoles in the saturated phase. In contrast, the ordering of the alkyl chains in the 1-butanol monolayers is significantly enhanced as compared to that in the neat 1-butanol phase. In addition to a surface excess of 1-butanol for both the saturated water and the 1-butanol phases, there is a subsurface layer that is depleted in 1-butanol molecules in these saturated phases. The formation of the surface monolayer (excess) and the depletion layer can be rationalized by the fact that the monolayer structure is mutually beneficial for water and 1-butanol because surface water possesses excess free hydrogens, while 1-butanol has excess hydrogen-bond acceptors. Once the surface excess of 1-butanol is formed, it results in an excess of hydrogen-bond acceptor sites in the subsurface layer which makes this a particularly favorable location for water molecules.

Acknowledgment. We thank Fiona Case and Sami Karaborni for stimulating discussions. Financial support from the National Science Foundation CTS-0138393 (J.I.S.) and CHE-0205146 (M.L.K.) is gratefully acknowledged. Part of the computer resources were provided by the Minnesota Supercomputing Institute.

JA027130N

(22) (a) Chang, T.-M.; Dang, L. X. *J. Chem. Phys.* **1996**, *104*, 6772. (b) Chen, B.; Xing, J.; Siepmann, J. I. *J. Phys. Chem. B* **2000**, *104*, 2391.